August 1986 LRP 294/86

CENTRAL MASS AND CURRENT DENSITY MEASUREMENTS IN TOKAMAKS USING THE DISCRETE ALFVEN WAVE SPECTRUM

G.A. Collins, A.A. Howling, J.B. Lister
and Ph. Marmillod

submitted for publication in

PLASMA PHYSICS AND CONTROLLED FUSION

CENTRAL MASS AND CURRENT DENSITY MEASUREMENTS IN TOKAMAKS USING THE DISCRETE ALFVEN WAVE SPECTRUM

G.A. Collins, A.A. Howling, J.B. Lister, Ph. Marmillod

Centre de Recherches en Physique des Plasmas
Association Euratom - Confédération Suisse
Ecole Polytechnique Fédérale de Lausanne
21, Av. des Bains, CH-1007 Lausanne / Switzerland

Abstract

The spectrum of global eigenmodes of the Alfvén wave for $\omega<\omega_{ci}$ offers the possibility of a very simple method for diagnosing the centre of a tokamak plasma. The frequencies of these modes depend on the central mass density and the current profile, and can be adequately estimated by MHD theory in cylindrical geometry including ion cyclotron effects. A simple unshielded bar antenna has been used to launch the waves at a power level of a few watts, detected by magnetic field probes in the boundary layer. Applications investigated on the TCA and PETULA tokamaks include estimates of the core current density over a wide variety of discharges, measurements of changes of the effective mass during impurity puffing and the observation of profile changes during sawtooth activity. A method for the measurement of the deuterium-tritium ratio in a tokamak is proposed.

1. INTRODUCTION

The current density profile in a tokamak plasma, which is one of the most important parameters in theories of confinement, stability and transport, remains one of the more elusive parameters to measure. Despite the recent successes of McCORMICK et al. (1985) (using the Zeeman splitting of atomic levels in an injected lithium beam) and SOLTWISCH et al. (1984) (using the Faraday rotation of a far-infrared laser beam), the value and variations in the current density profile $j(r)$ near the axis can only be indirectly inferred. Many other methods have also been proposed and tested (see, for example, PEACOCK (1979) and EQUIPE TFR (1978)), none of which are in regular use.

The mass density of a tokamak plasma is even less well known, since no direct measurement has previously been developed. The effective mass $A_{eff}=\sum\eta_i A_i$ (where $\eta_i=n_i/n_e$ is the concentration of the ion state with mass A_i and charge Z_i, such that $\Sigma\eta_i Z_i=1$) must be inferred by measurements of Z_{eff}, or from the spectroscopic determination of impurity influxes.

In this paper we discuss the use of the global eigenmode of the Alfvén Wave, referred to as the Discrete Alfvén Wave (DAW), to obtain information on both of these important parameters. The DAW spectrum requires little interpretation to determine the effective mass at the axis; the technique is simple in concept and is easily implemented. For central current densities the interpretation is more difficult although the DAW spectrum can be very sensitive to small changes in the current profile.

The outline of this article is as follows. Section 2 provides a brief description of the theoretical background. Section 3 discusses the installation of this diagnostic and includes results obtained on the TCA and PETULA tokamaks. Section 4 discusses the effective mass diagnostic together with results from the TCA tokamak during impurity puffing, and Section 5 provides the basis for a deuterium-tritium mixture ratio measurement. In section 6 we develop the analysis of the central current density measurement.

2. THEORETICAL BACKGROUND

The excitation of Shear Alfvén Waves is being studied on the TCA tokamak (R,a = 0.61, 0.18 m, $B_0 \leq 1.5$ T, $I_p \leq 170$kA). A detailed description of the results of the antenna loading and vacuum wavefield measurements has been given by COLLINS et al. (1986). The experimental data clearly indicate features due to both DAW resonances and the Shear Alfvén Wave continua. The continua are defined in the large aspect ratio approximation by

$$\omega_A^2(r) = (n+m/q(r))^2 \cdot B_0^2 \cdot (1-\omega^2{}_A/\omega_{ci}^2)/(\mu_0 \rho(r) R_0^2) \qquad (1)$$

in which (n,m) are the toroidal and poloidal mode numbers, q(r) and $\rho(r)=n_e(r)A_{eff}m_p$ are the local safety factor and mass density, B_0 and R_0 are the toroidal magnetic field on axis and the major radius. Each continuum labelled by (n,m) has a minimum value ω_{min} (the threshold frequency) which can be on- or off-axis. The direct measurement of the continuum using phase contrast interferometry (BEHN et al. (1986)) can be used to determine the local parameters. The

complexity of this measurement, however, has prevented its routine use. The DAW resonances are, on the other hand, readily identified by peaks in the antenna loading and the rf magnetic wavefield amplitude, and by fast rotation of the rf wavefield phase. They occur at frequencies below the threshold frequency ω_{min}, with the dominant mode for each (n,m) being the first radial eigenmode whose frequency ω_1 is furthest from the continuum. Even so, ω_1 is close to the resonant frequency on axis $\omega_A(0)>\omega_{min}$ and this fact led to the proposition that these eigenmodes could be used to determine q(0) and $\rho(0)$ (JOYE et al. (1981)). In reality, because the DAW is a global eigenmode, the separation $\Delta\omega = \omega_A(0)-\omega_1$ depends sensitively on the profiles of $\rho(r)$ and q(r),but it can be calculated. While some approximations exist to estimate $\Delta\omega$ in restrictive conditions, we prefer to calculate ω_1 directly using a 1-D code which includes the equilibrium current and $\omega/\omega_{ci}\neq 0$. APPERT et al. (1985) showed that this model is adequate in predicting the DAW frequencies, even for those modes which are excited indirectly by toroidal coupling.

Global modes of the fast wave have frequencies which depend on global parameters, such as the average mass density, but, as their popular name "cavity mode" implies, their frequencies are sensitive to the boundary conditions. Although BRENNAN, McCARTHY and SAWLEY (1980) and HOWELL and CAYTON (1982) have discussed this diagnostic, it has not been used on a tokamak except for the preliminary experiments of HAHNEKAMP and STAMPA (1981). The theoretical sensitivity of the DAW spectrum to changes in the central parameters has motivated this present study.

3. IMPLEMENTATION OF THE DIAGNOSTIC

The observation of the DAW spectrum by De CHAMBRIER et al. (1982a) and its detailed study by COLLINS et al. (1986) made use of the full set of eight antenna groups installed on TCA for Alfvén Wave Heating experiments. The first measurements of current profile modulation were made by De CHAMBRIER et al. (1982b) using this antenna system. The frequency, however, was fixed, and such a complex antenna system precludes the general use of such a diagnostic.

We have developed a simple flexible system on TCA using a single floating unshielded antenna at the bottom of the plasma, subtending a poloidal angle of 90° and comprising two 10 mm diameter parallel bars 70 mm apart. On PETULA (R,a = 0.71, 0.17 m, B_0=2.8T) a similar unshielded antenna was used, grounded at one end, and positioned at the outer midplane. A 200W amplifier provided 1 - 5 Amperes of antenna current via a wideband matching circuit covering 2 - 12 MHz, shown in Fig. 1. A magnetic field probe, placed inside a ceramic tube in the scrape-off plasma 180° toroidally from the antenna and at the top of the torus, detected either the toroidal or poloidal component of the driven mode on PETULA. The probe was at Ø=135° on TCA, and at the outer midplane. A heterodyne detection system allows an excellent signal to noise ratio with less than 10W coupled to the plasma. We measure the in-phase and in-quadrature components of the antenna current and the rf wavefield using the system shown schematically in Fig. 2. This is achieved by splitting the reference signal into two components $\pi/2$ out of phase, which are then separately mixed with the detected signals. The combination of only one antenna and only one

probe cannot selectively excite or detect any particular mode. All DAWs are therefore detected when resonant. Experiment and theory have shown that for $\omega/\omega_{ci}<0.5$, only those DAWs with $m/n\geq 0$ can be excited, while COLLINS et al. (1986) found that the dominant peaks have poloidal mode number $m=-1$ and toroidal mode numbers $n<0$. In toroidal geometry, n remains a pure description of the mode, whereas the modes are no longer pure harmonics of the poloidal angle. However, we continue to use the m number as a label for the corresponding cylindrical mode, which remains the most important component.

Figure 3 shows a typical frequency scan of the toroidal rf wavefield on PETULA. The pronounced peaks correspond to different values of $|n+m|$, since in general $q(0)\sim 1$ (see Eq. 1). The phase angle between the antenna current and the detected rf wavefield increases at each resonance. As a first check of this diagnostic method, the plasma density on PETULA was varied from $1\rightarrow 5\times 10^{19} m^{-3}$ and a 2 - 9 MHz frequency scan was performed during the flat-top of each discharge, with a sweep time of ~30 msec. On TCA the frequency scan was from 1.5 - 4.5 MHz for a wider density range. In Fig. 4 the observed DAW peaks are shown as points, and the curves derived from the 1-D model are shown as solid lines. The agreement between theory and experiment is excellent for PETULA, but there is a systematic error of a few percent for TCA, which we attribute to a small error in the toroidal field measurement.

Instead of repetitively scanning the driving frequency using a sawtooth ramp, we have operated with a phase-locked loop on one DAW at a time, thereby increasing the frequency resolution significantly

although the spectral information is reduced. This is done by first scanning the frequency across the DAW resonance to identify whether the zero-crossing of the cosine or sine component of the b_ϕ signal (see Fig. 2) is closest to the resonance peak. The DAW is then followed during subsequent shots using a frequency correction feedback to maintain the chosen component at zero amplitude. In this way the DAW is tracked to within a phase margin of $\pi/2$ of the resonance peak. Figure 5 shows the temporal evolution of the DAWs with $|n+m| = 2, 3, 5$ and 6 during Lower Hybrid Current Drive (LHCD) experiments on PETULA using this method of frequency tracking.

The modulation of the DAWs by the sawtooth activity, reported by De CHAMBRIER et al. (1982b), has been confirmed using the phase sensitive system. In Fig. 6 the frequency was swept slowly over an extremely narrow frequency range to emphasise the change of DAW frequency as revealed by the detected phase. The phase modulation clearly indicates that the amplitude modulation must be attributed to a resonant frequency variation, and not simply to a change in the excitation strength.

These results show that the excitation and detection of the DAWs can easily be implemented in a tokamak using a low power rf supply, a simple unshielded antenna and an rf pickup coil inside the vacuum vessel.

4. EFFECTIVE MASS ESTIMATION

Equation 1 shows that the Alfvén wave spectrum is sensitive to

the effective mass of the plasma. Assuming that the effective mass does not vary as a function of radius, the value of $\omega_1 \approx \omega_A(0)$ should scale as $A_{eff}^{-0.5}$. When the finite frequency and the separation $\Delta\omega$ between the DAW and the continuum are taken into consideration this relationship is modified. We have calculated the resonant frequencies for three DAWs in TCA conditions, with (n,m) = (-2,-1), (-3,-1) and (-4,-1), for different impurity concentrations and impurities. The profiles of the safety factor and density were not changed and the impurity concentration was taken to be constant over the whole plasma volume. The results of these calculations, Fig. 7, show the modified form of the relationship

$$A_{eff} = \text{const.} \times V_{A_H}^{1.67} \; \omega_1^{-1.87} \qquad (2)$$

in which V_{A_H} is the central value of the Alfvén speed, taking $n_i = n_e$, and the discharge to be pure hydrogen, i.e.

$$V_{A_H} = 6.89 \times 10^6 \times B_0(T)/\{n_e(0)/10^{19}\}^{0.5} \text{m/sec} \qquad (3)$$

Equation 2 can be rewritten as

$$\omega_1 = \text{const.} \times V_{A_H}^{0.89} \times A_{eff}^{-0.53} \qquad (4)$$

clearly showing the departure from the simple model. The spread in the generated data is small even though the impurity type was varied. The slopes of the lines are given to a few percent by $|n+m|^{1.87}$, as expected from Eq. 2.

The results of Fig. 7 were generated using fixed radial profiles of density and current. Figure 8 shows the variation in ω_1 for seven DAW resonances, when the profiles were varied for PETULA plasmas (deuterium, $\bar{n}_e = 3 \times 10^{19} m^{-3}$, q(a)=3.76). The family of profiles chosen was

$$\rho(r) = \rho_o(1-r^2/a^2)^{\alpha_\rho} \quad ; \quad j(r) = j_o(1-r^2/a^2)^{\alpha_j}, \qquad (5)$$

where $\alpha_j = q(a)/q(o)-1$.

When α_ρ is varied, the variation in frequency is small and could be accounted for if the density profile were accurately measured. If the radial profile of A_{eff} were to vary, the gradients of these curves give an indication of the expected error in the estimation of $A_{eff} \sim \omega_1^{-1.87}$, which is only a few per cent. This question is developed further in Section 5.

We have exploited this diagnostic in a series of discharges in TCA with different gas compositions, see Fig. 9. With deuterium as the filling gas the measured value of A_{eff} was always close to 2.0. With a plasma current of 130 kA the central electron temperature was ~700-800 eV, and low-Z impurities, mainly carbon, are fully stripped. Since the ratio A/Z for light, fully-stripped ions is always ~2.0, we see why A_{eff} is independent of the electron density even if Z_{eff} decreases as the density increases. The lower curve, labelled 'H-only', is the variation in A_{eff} as a function of $\bar{n}_e$ when hydrogen is used as the filling gas. At high density we are close to A_{eff}=1.0 whereas at low density, $\bar{n}_e < 2 \times 10^{19}$ m^{-3}, A_{eff} is around 1.3, indicating an increase in the impurity concentration. If

we assume that the dominant impurity is carbon, we obtain η_{carbon} = 5 %; if it were oxygen, then η_{oxygen} = 3.75 %. The corresponding values of Z_{eff} are 1.7 and 3.1 respectively.

A series of hydrogen filling discharges with a target plasma of $\bar{n}_e = 1.8 \times 10^{19}$ m^{-3} was used for impurity puffing experiments. The electron density was increased by up to a factor of 3 using nitrogen injection. The results are labelled 'N → H' in Fig. 9. The value of A_{eff} for these discharges is far higher than the hydrogen filling discharges with the same electron density. The curve labelled '+100 %' is the calculated value of A_{eff} if the increased density is due to fully stripped nitrogen. It lies well above the experimental data points, which are fitted by the curve labelled '+50 %', obtained if we assume that 50 % of the electron density increase is due to the fully stripped injected impurity and 50 % is from hydrogen. The reason for this is uncertain. The injected impurity may increase the hydrogen recycling at the wall, but there is no increase in the H_α emission. The alternative explanation is that there is an increase in the confinement of the hydrogen ions due to changes in the discharge condition as a result of the impurity puffing - this might be related to the "Z mode" behaviour on the ISX-B tokamak (LAZARUS et al. (1985)).

5. MEASUREMENT OF THE D-T MIXTURE

Since this effective mass diagnostic is so sensitive, it can be used to measure the tritium concentration in a D-T mixture, for which no other direct measurement is available. The average mass of the deuterium plus any fully stripped impurities will be 2.0, so we obtain

the fraction of tritium added, equal to

$$\eta_T = A_{eff} - 2.0 \qquad (6)$$

even in the presence of impurities. Modelled curves for tritium puffing are labelled "T→D" in Fig. 9. As a result of the interest in this method, we have performed a detailed sensitivity analysis for this particular case.

We shall consider the possible errors in measuring the D-T ratio for the case in which the concentrations are given to be equal on axis, i.e. $A_{eff}(0)=2.5$. It may be assumed that the electron density profile $n_e(r)$ is accurately measured, and that the current profile has the form of Eq. 5; the size of the errors due to any uncertainty in these profiles can be estimated from Fig. 8. The dependence of the DAW frequency on these profile changes is weak in comparison with the effective mass relation in Eq. 2.

The most important unknown is the radial distribution of the relative D-T concentration which may not necessarily be constant during tritium fuelling. We have parameterised a range of radial mass distributions by assuming a parabolic electron density profile, with different profiles of deuterium or tritium density of the form in Eq. 5. The resulting mass density profile is

$$\frac{\rho(r)}{\rho(0)} = \frac{1}{2.5}\,(1-r^2/a^2)\left\{\begin{array}{c} 3 - {}^1/_2(1-r^2/a^2)^{\alpha_D-1} \\ 2 + {}^1/_2(1-r^2/a^2)^{\alpha_T-1} \end{array}\right\} \qquad (7)$$

giving $A_{eff}(0)=2.5$, where deuterium or tritium respectively has the radial number density profile characterised either by α_D or α_T. Figure 10 illustrates the different density profiles examined for

which the changes in the estimate of the effective mass and the consequent error in the estimation of the tritium concentration on axis are given in Fig. 11. This analysis was performed for m=-1 and n =-1 to -7 and shows that n =-4 to -7 have approximately the same sensitivity to the unknowns α_D and α_T and also lead to the minimum error in the estimate. These figures show that over a wide range of concentration profiles, the error in estimating $A_{eff}(0)$ is only a few percent. The diagnostic is therefore primarily sensitive to $A_{eff}(0)$ and independent of the radial concentration distribution for this range of toroidal mode numbers, n =-4 to -7. As a result of these tests, we conclude that the measurement of the D-T mixture using this method is extremely promising.

6.ESTIMATION OF CENTRAL CURRENT DENSITY

The frequency of the continuum resonance on axis, $\omega_A(0)$, yields the value of the safety factor on axis, q(0). The separation of the DAW from this frequency, $\Delta\omega$, greatly confuses this simple picture. Figure 12 shows this from a series of calculations for PETULA in which α_n was held constant and α_j was varied, with the parametrisation of Eq. 5. The computations have been made for m = -1 and -2 and for n =-1 to -4. The solid line is the DAW frequency, the dashed line is $\omega_A(0)$ and the dotted line is ω_{min}. The onset of non-monotonic frequency profiles ($\omega_{min}<\omega_A(0)$) is clearly seen for the different n, m and q(0). This is most evident for m=-1 and low $|n|$, and further increases $\Delta\omega$ which reduces the sensitivity of ω_1 to q(0). This makes the use of low $|n|$ DAWs as a q(0) diagnostic more difficult compared with the cases in which $\omega_1 \sim \omega_A(0)$. From these curves, a differential

sensitivity $\delta\omega_1/\delta q(0)$ could be found for each mode and we might then in principle deduce q(0). Figure 12 (b) indicates that if m=-2 modes could be separated from the mode mixture which occurs at any given value of $|n+m|$, then even the low $|n|$ modes could be used.

Due to the complexity of the origins of the separation $\Delta\omega$, this picture is dependent on the model chosen for the current profile. The "α_j-model" of Eq. 5 is convenient but is extremely restrictive, allowing no variation in the current profile width for a given value of q(0). We have therefore used an alternative parametrisation

$$j(r) = j_0(1- \frac{r^\beta}{a^\beta})^\gamma \qquad (8)$$

in which j_0 defines q(0), and β, γ define together q(a) and a profile width. Figure 13 shows the variation in ω_1 for the same conditions as Fig. 12, with q(0) = 1 and β as a free parameter; β = 2 corresponds to the previous case. The eigenmode frequency depends on β and is therefore not trivially related to q(0). There can therefore be many current profiles which give the same resonant frequency for a particular eigenmode. Figure 14 illustrates this further with three sets of current density profiles; each pair of curves represents profiles parametrised by Eqs. 5 and 7 for which the (n,m)=(-2,-1) DAW has the same frequency. Figure 15 shows that the general form of the current profile, as characterised by l_i and q(r=a/2) is well defined by the DAW frequency although a precise value of j(0) (and hence q(0)) is clearly not obtained. In principle, the resonant frequencies of several eigenmodes could be used to discriminate between the range of possible current profiles, thereby allowing an estimate of q(0). However we have found that the absolute value of the DAW frequencies would have to be known to within 0.3%. While this precision is

possible for the frequency measurement, the uncertainty due to toroidal effects in the theoretical calculations and experimental parameters means that this discrimination is not realistically achievable. The eigenfrequencies, then, do depend on the current profile and can yield an estimation of the parameters in Fig. 15, but q(0) is not easily obtainable, especially for $q(0)<1$ where $\Delta\omega$ becomes large. We can say that $q(0)\sim1$ does give a good fit for the experimental data of Figure 4 (for which we assumed the current profile of Eq. 5), but without further information on the current profile type, the value of q(0) remains ambiguous within an error margin of ± 30% for the profile types investigated here.

We now turn to the experimental results concerning the current profile sensitivity. De CHAMBRIER et. al. (1982b) showed that in some cases the sawtooth modulation could only be ascribed to a modulation of the current profile. The slow frequency sweep in Fig. 6 is an example in which the sign of the phase modulation is that predicted by a density modulation. Figure 16 shows the frequencies of the DAWs $n = -2, -3, -4$ and $m = -1$ for a current scan from $q(a) = 10$ to 2.6. The data points are compared with the curves generated from the measured density profiles, assuming constant effective mass (D_2 operation). The experimental points cross the constant current profile curves, generated from the α_j parametrisation, showing that the current profile is varying as a function of q(a), increasing the current density in the core as q(a) decreases. The experimental points cross the $q(0) = 1$ curve at $1/q(a) = 0.21$ at which point the sawtoothing activity was seen to begin.

In order to test different types of profiles at constant plasma current, the plasma current in TCA was ramped at different rates, crossing I_p = 98 kA (q(a)~4). Figure 17 shows that the DAW frequency varied as the ramp rate varied from -0.7 to 11.0 $MAsec^{-1}$, in the sense that for positive ramp rates the frequency was lower, corresponding to a lower central current density (see Fig. 15), as expected from classical diffusion.

We conclude that there are several experimental features which illustrate the sensitivity of the DAW spectrum to changes in the current profile, as predicted by numerical claculations.

7. DISCUSSION

We have introduced the principles underlying the use of Global Eigenmodes of the Alfvén Wave as a plasma diagnostic yielding information on the plasma mass and plasma current profile. The diagnostic was installed on the TCA and PETULA tokamaks in a primitive form to demonstrate the technical simplicity and ease of operation. A major improvement to this system would be the use of two magnetic field probes180° apart toroidally, to select modes with odd and even toroidal mode numbers thus allowing the separation of m=-2 modes (which are more sensitive to profile changes) from the mode mixture which occurs at any given value of $|n+m|$. This would also provide a much cleaner signal for tracking, and would confirm the mode identification. Several peaks could be tracked simultaneously using separate phase-locked-loops but with the same antenna and magnetic field probes. The use of the diagnostic for effective mass measurements is straight for-

ward, would need little refining, and could be implemented to measure the D-T mixture ratio and control it inside a feedback loop.

The use of the diagnostic for current profile measurements is less obvious. The DAW spectrum contains information on the current profile, but not in such a simply extractable form as hoped. The preliminary results obtained on the PETULA tokamak showing detailed variations during the LHCD rf pulse underline the importance of understanding the dependence on the current profile.

Acknowledgements - It is a pleasure to acknowledge the contributions of the PETULA Team in proposing that we install this diagnostic on PETULA, and in aiding with its implementation, particularly Drs. F. Parlange and J.-C. Vallet. We are grateful for the encouragement of Prof. F. Troyon and the assistance of T. Dudok de Wit in carrying out this study, which was partly funded by the Fonds National Suisse de la Recherche Scientifique.

REFERENCES

APPERT K., COLLINS G.A., HOFMANN F., KELLER R., LIETTI A., LISTER J.B., POCHELON A. and VILLARD L. (1985) Phys. Rev. Letts 54, 1671.

BEHN R., COLLINS G.A., LISTER J.B. and WEISEN H. (1986) Proc. 13th European Conf. on Controlled Fusion and Plasma Heating, Schliersee.

BRENNAN M.H., McCARTHY A.L. and SAWLEY M.L. (1980) Plasma Phys. 22, 77.

De CHAMBRIER A., CHEETHAM A.D., HEYM A., HOFMANN F., JOYE B., KELLER R., LIETTI A., LISTER J.B. and POCHELON A. (1982a) Plasma Phys. 24, 893.

De CHAMBRIER A., DUPERREX P.-A., HEYM A., HOFMANN F., JOYE B., KELLER R., LIETTI A., LISTER J.B., POCHELON A. and SIMM W.C. (1982 b) Phys. Lett. 92A, 279.

COLLINS G.A., HOFMANN F., JOYE B., KELLER R., LIETTI A., LISTER J.B. and POCHELON A. (1986) Phys. Fluids, 29, 2260.

EQUIPE TFR (1978) Nucl. Fus. 18, 647.

HAHNEKAMP H.G. and STAMPA A. (1981) Plasma Phys. 23, 845.

HOWELL R.B. and CAYTON T.E. (1982) Plasma Phys. 24, 1051.

JOYE B., LIETTI A., LISTER J.B. and POCHELON A. (1981) "Discrete Alfvén Wave excitation as a tokamak plasma diagnostic", LRP 196/81, Lausanne.

LAZARUS E.A. et al. (1985) Nucl. Fusion 25, 135.

McCORMICK K. et al. (1985) Proc. 12th European Conference on Controlled Fusion and Plasma Heating, Budapest, Vol. 1, 199.

PEACOCK N.J. (1979) in "Diagnostics for Fusion Experiments" ed. E. Sindoni and C. Wharton, Commission of the European Communities, Luxembourg, 367.

SOLTWISCH H., GRAFFMAN E., SCHLUTER J. and WAIDMAN G. (1984) Proc. Int. Conf. on Plasma Physics, Lausanne, Vol. 1, 499.

FIGURE CAPTIONS

Fig.1. a) Wideband matching circuit.

b) Equivalent circuit.

c) Frequency response.

Fig.2. Heterodyne detection system.

Fig.3. PETULA spectrum (I_p=147kA, $\bar{n}_e$ =3 × $10^{19}m^{-3}$).

Fig.4. Density scans - measurements and theory (m=-1 and q(0) is taken to be 1).

Fig.5. Frequency tracking during LHCD in PETULA.

Fig-6. Sawtooth modulation of DAWs in TCA (10kHz/ms, $|m+n|$=5, I_p=120kA, $\bar{n}_e$ = 3 × $10^{19}m^{-3}$).

Fig.7. Theoretical scaling law for A_{eff} (TCA parameters).

Fig.8. DAW frequency dependence on density and current profiles (see Eq. 5). Dashed line : α_ρ dependence; solid line : q(0) dependence.

Fig. 9. A_{eff} during impurity injection : "N→H"-nitrogen puffing into hydrogen, "T→D" tritium fuelling of a deuterium plasma.

Fig.10. Range of complementary density profiles of deuterium and tritium used in the sensitivity analysis.

Fig.11. Profile dependence error in the estimation of the tritium concentration on axis if $A_{eff} \sim \omega_l^{-1.87}$ is assumed, for a given concentration of 50% on axis.

Fig.12. Frequency dependence for $\omega_A(0)$ (dashed line), ω_{min} (dotted line) and ω_l (solid line) as the current profile form in Eq. 5 is varied, for m=-1 and -2.

Fig.13. Frequency dependences as in Fig. 12, for current profiles of the form in Eq. 8.

Fig.14. Possible current density profiles for given (n,m) = (-2,-1) eigenmode frequencies. Solid lines using Eq. 7; dashed lines, using Eq. 5.

Fig.15. Dependence of the (n,m)=(-2,-1) DAW frequency on $q(a/2)$ and l_i for the current density profiles of Fig. 14.

Fig.16. TCA current scan with curves from model profiles.

Fig.17. Change in (-2,-1) frequency with ramping current.

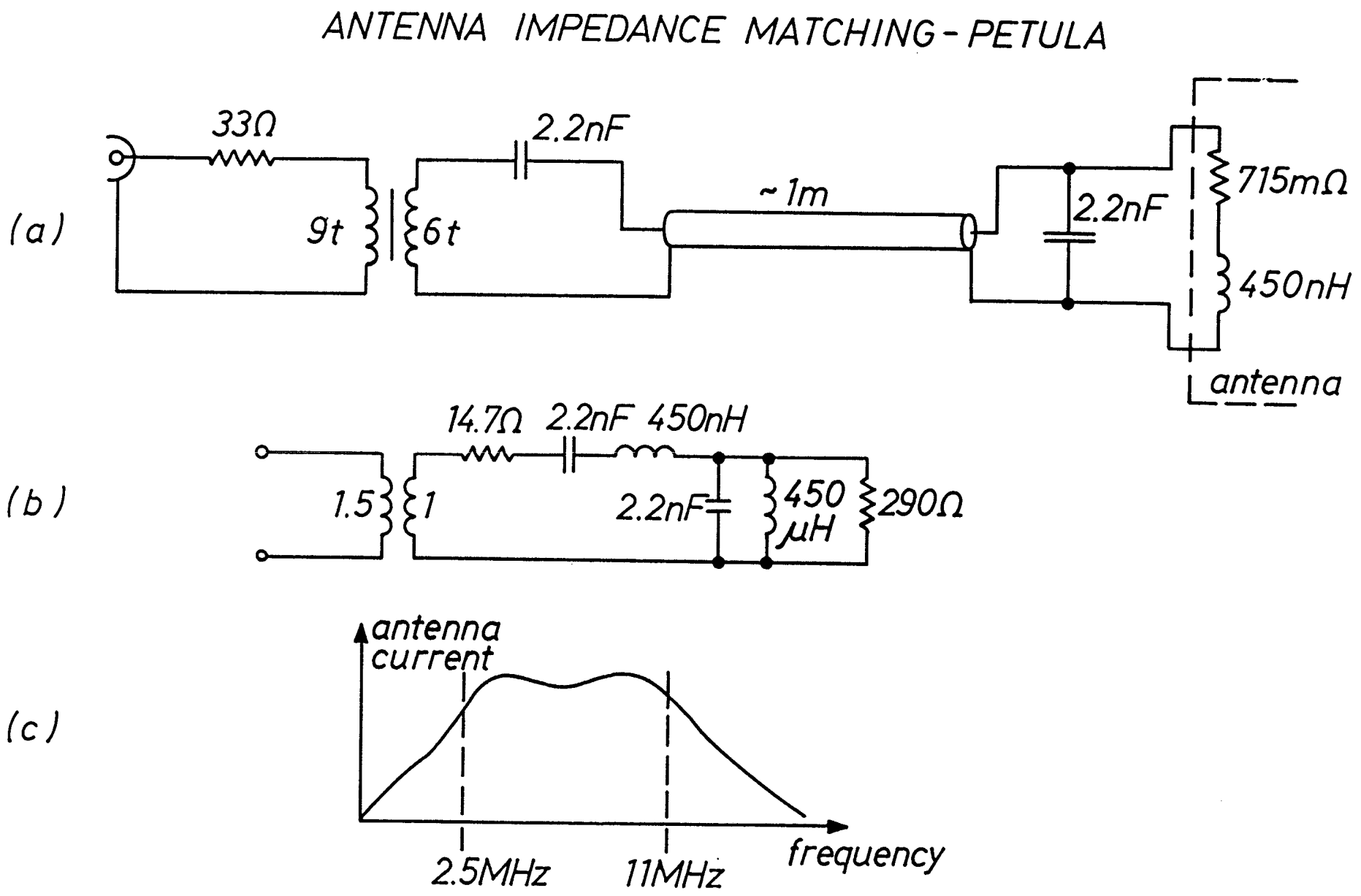
ANTENNA IMPEDANCE MATCHING - PETULA
(a)
33Ω
9t
6t
2.2nF
~1m
2.2nF
715mΩ
450nH
antenna
(b)
14.7Ω
2.2nF
450nH
1.5
1
2.2nF
450 μH
290Ω
(c)
antenna current
2.5MHz
11MHz
frequency

Fig. 1

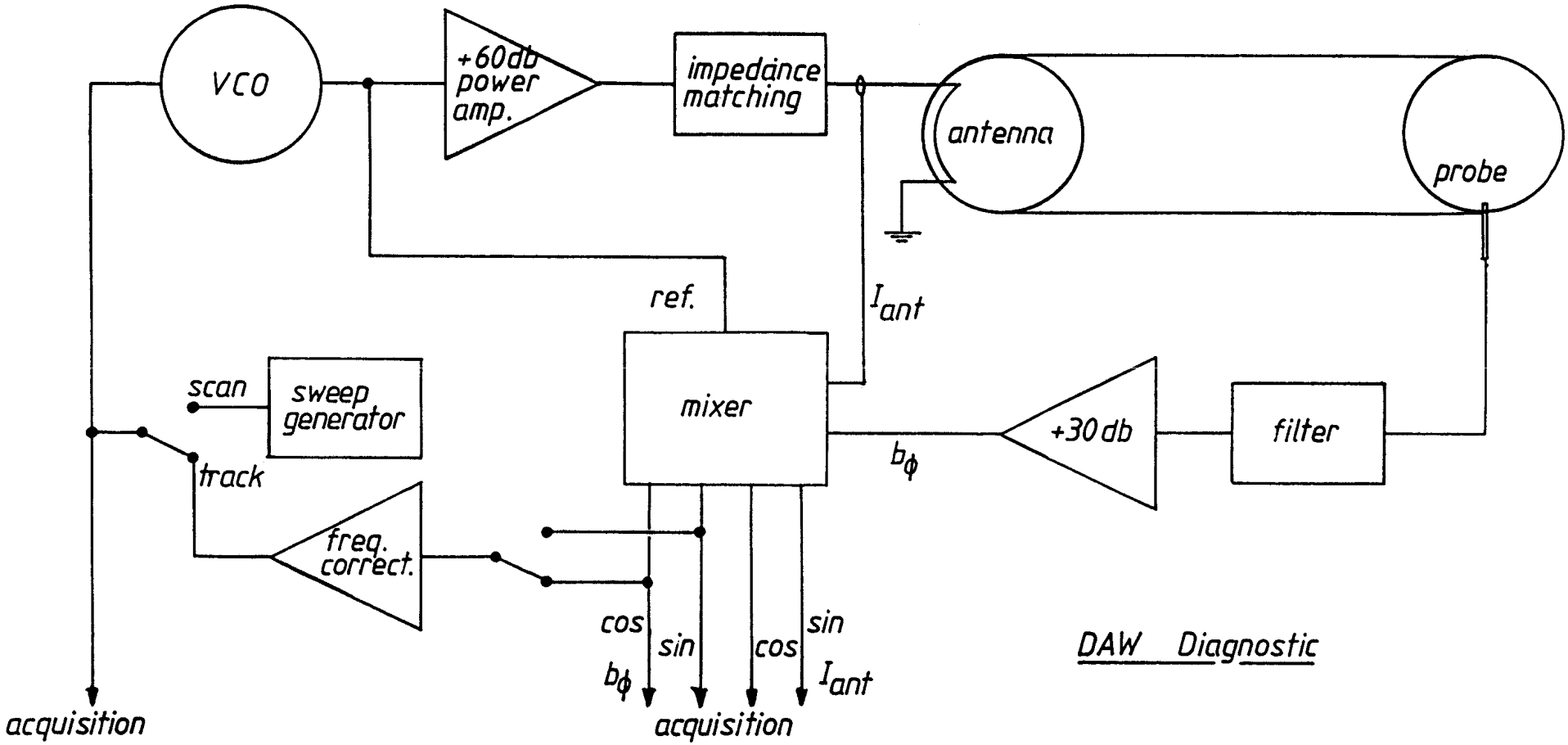
VCO
+60db power amp.
impedance matching
antenna
probe
ref.
I_{ant}
scan
sweep generator
mixer
+30 db
filter
track
b_ϕ
freq. correct.
cos
sin
cos
sin
b_ϕ
I_{ant}
acquisition
acquisition
DAW Diagnostic

FIG. 2

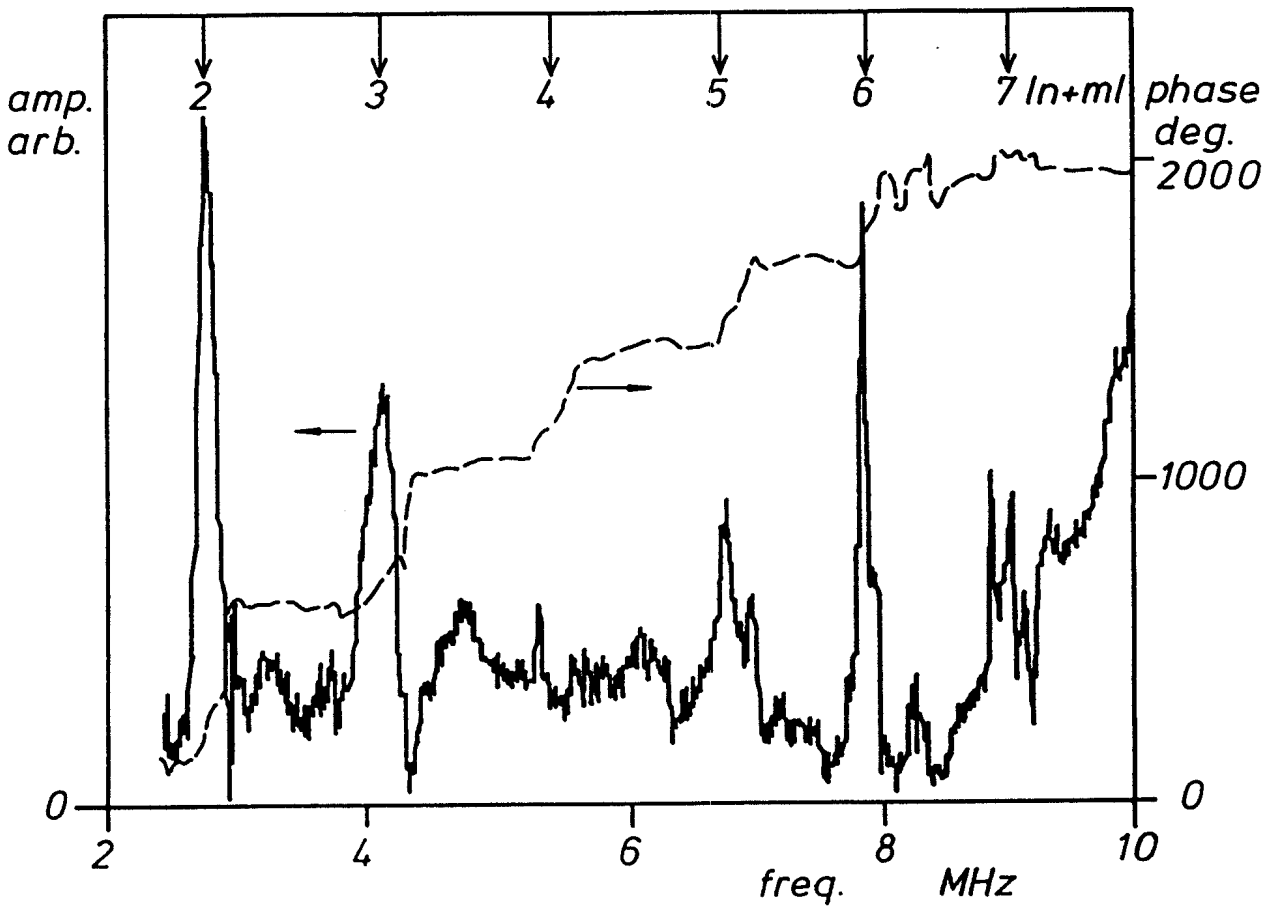

FIG. 3

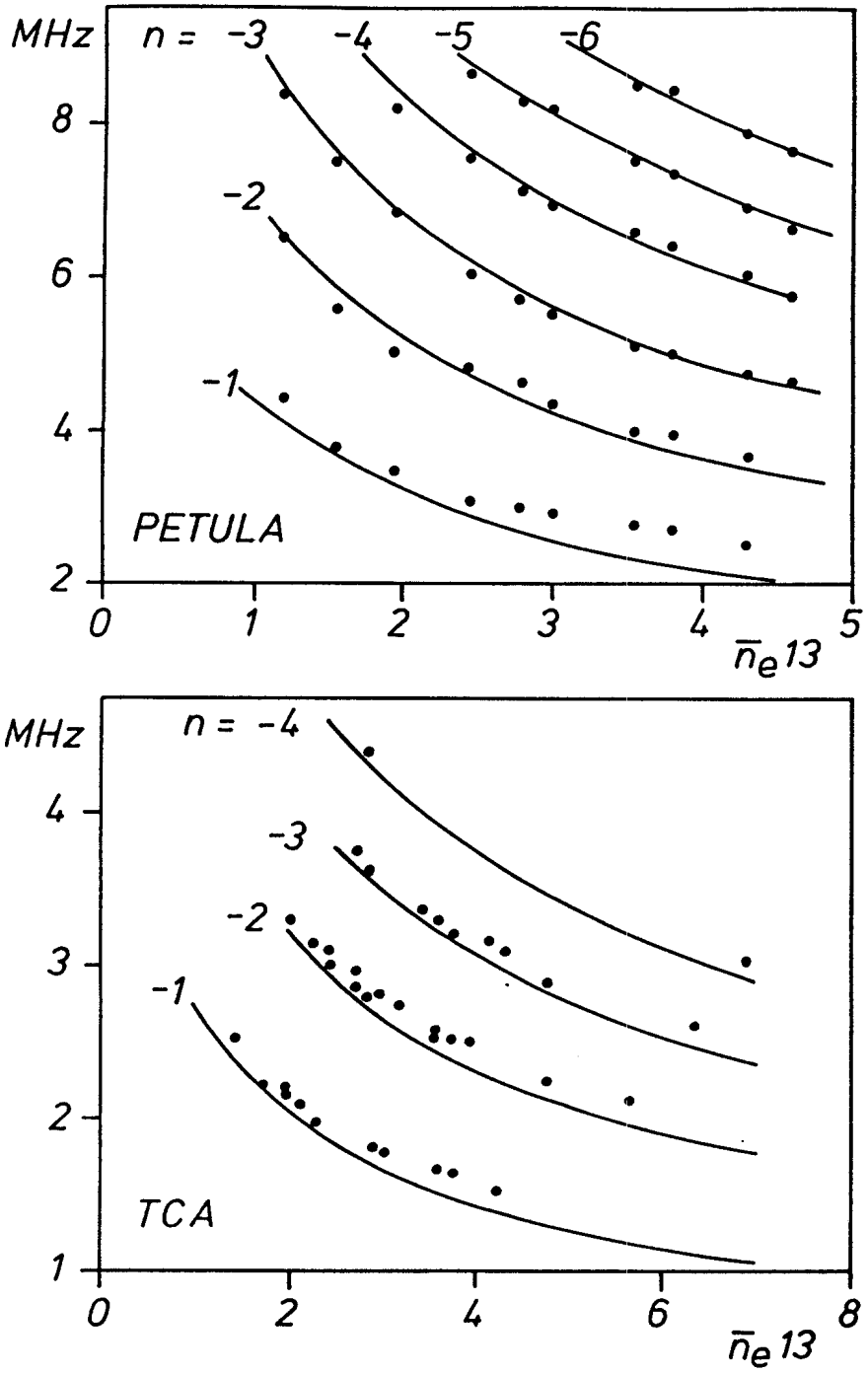
MHz
n = -3
-4
-5
-6
-2
-1
8
6
4
2
PETULA
0
1
2
3
4
5
$\bar{n}_e 13$
MHz
n = -4
-3
-2
-1
4
3
2
1
TCA
0
2
4
6
8
$\bar{n}_e 13$

FIG. 4

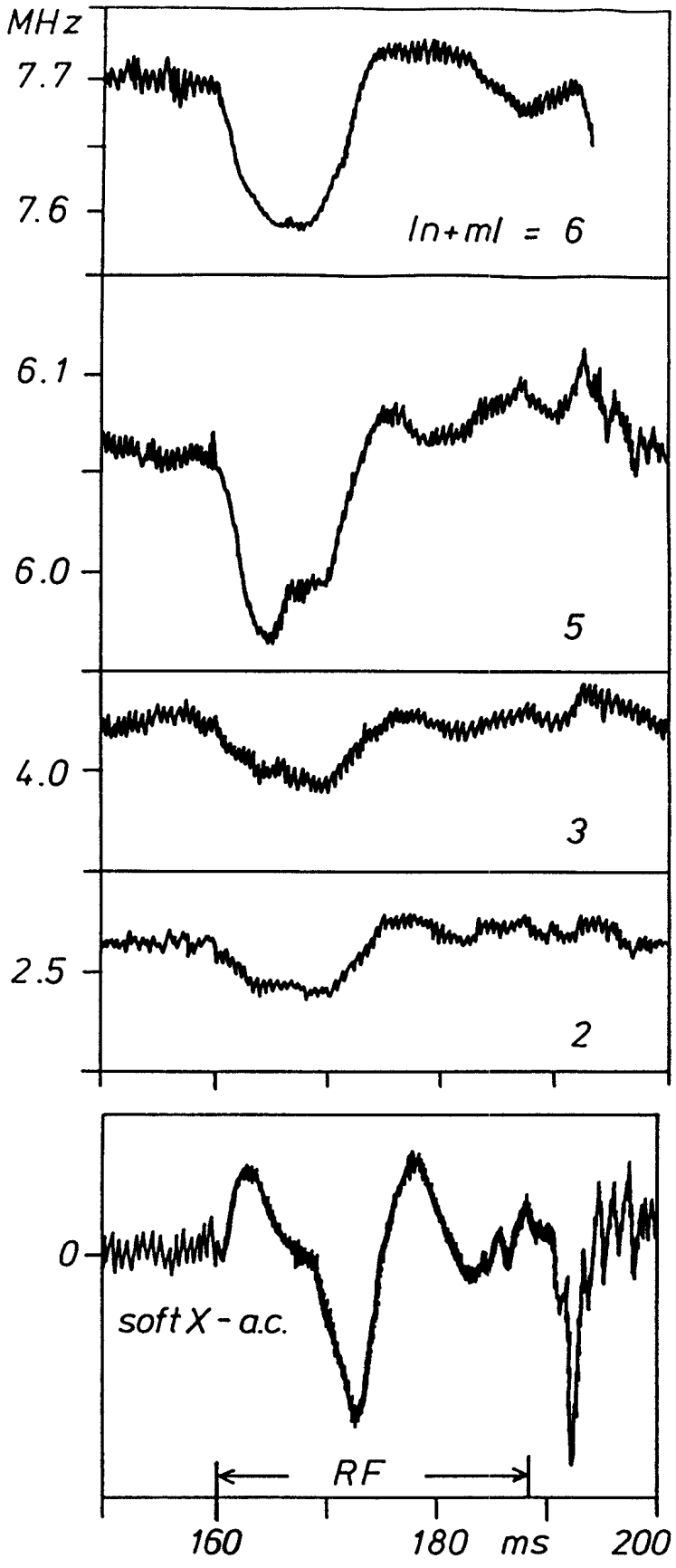

FIG. 5

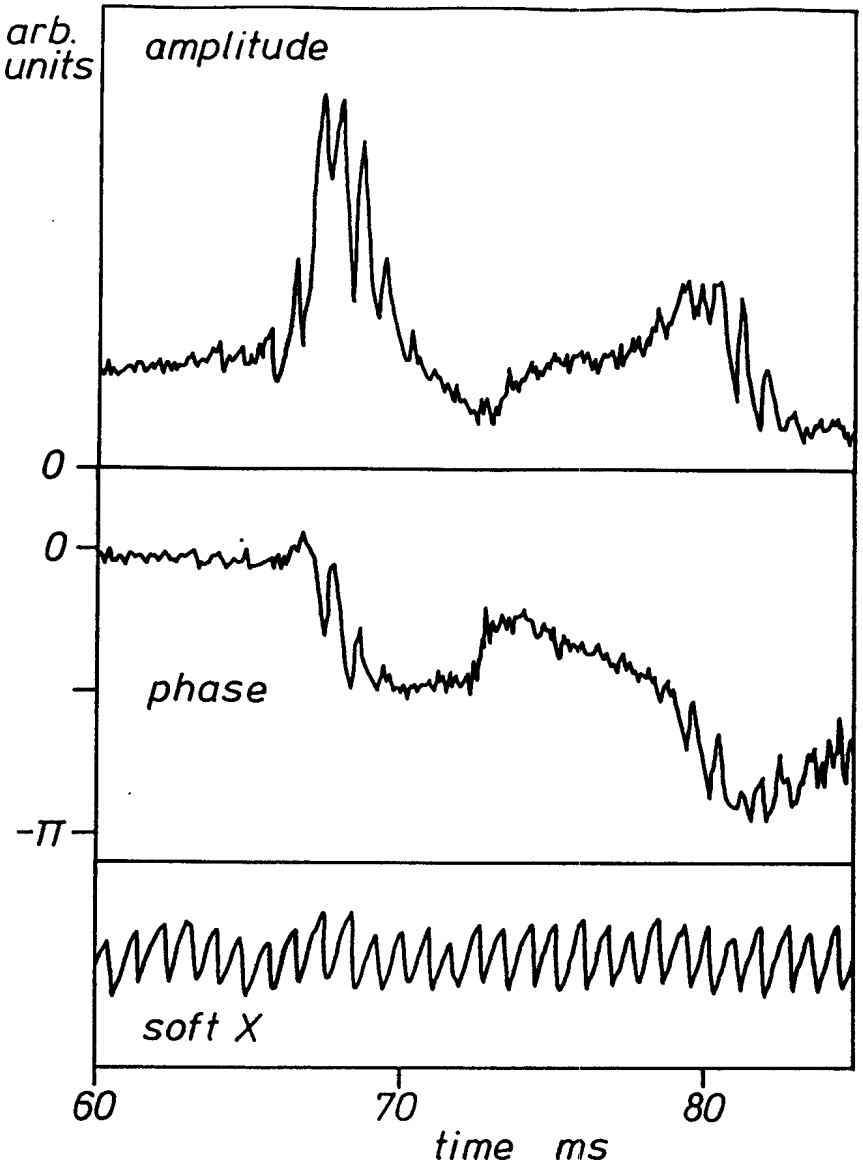

FIG. 6

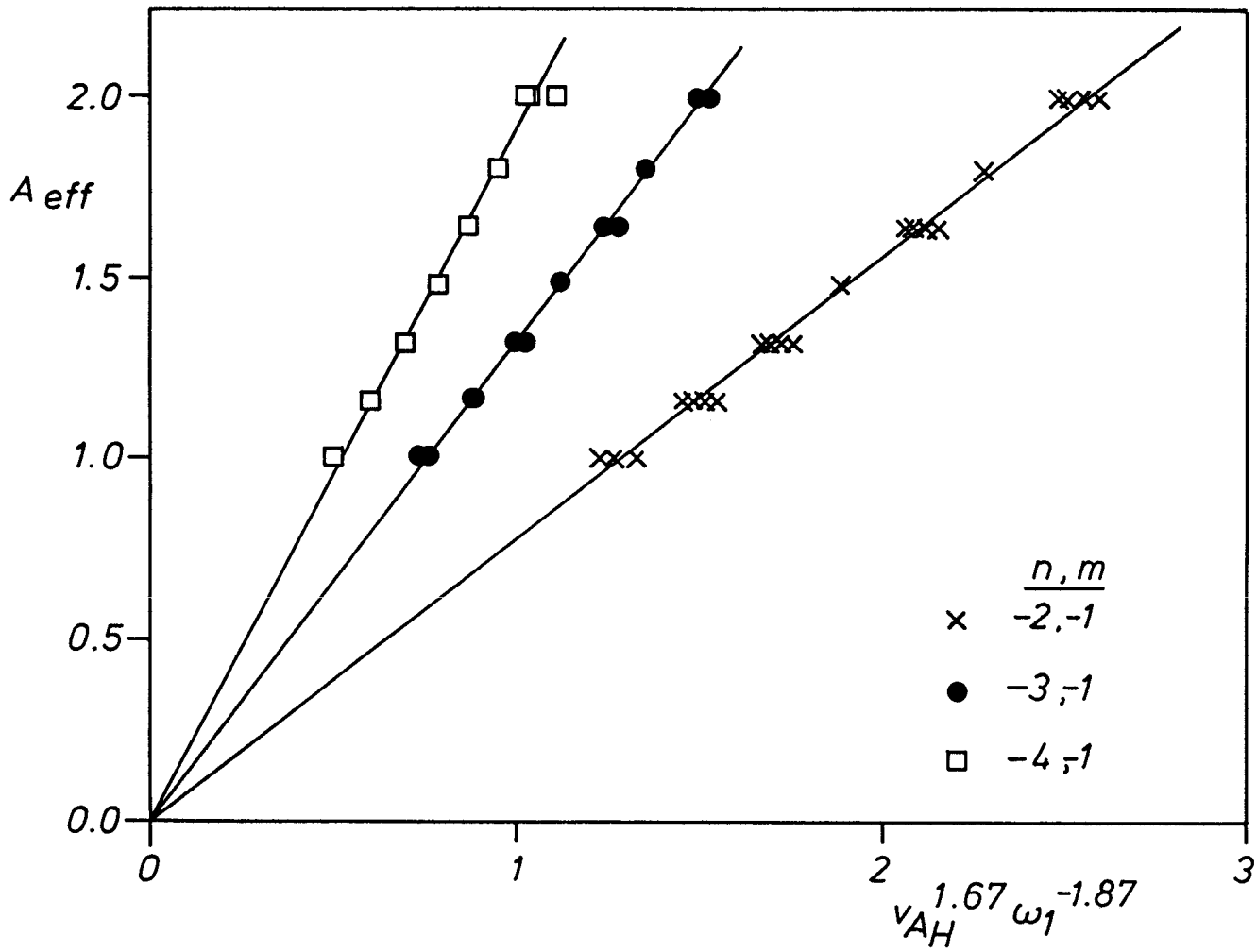

FIG. 7

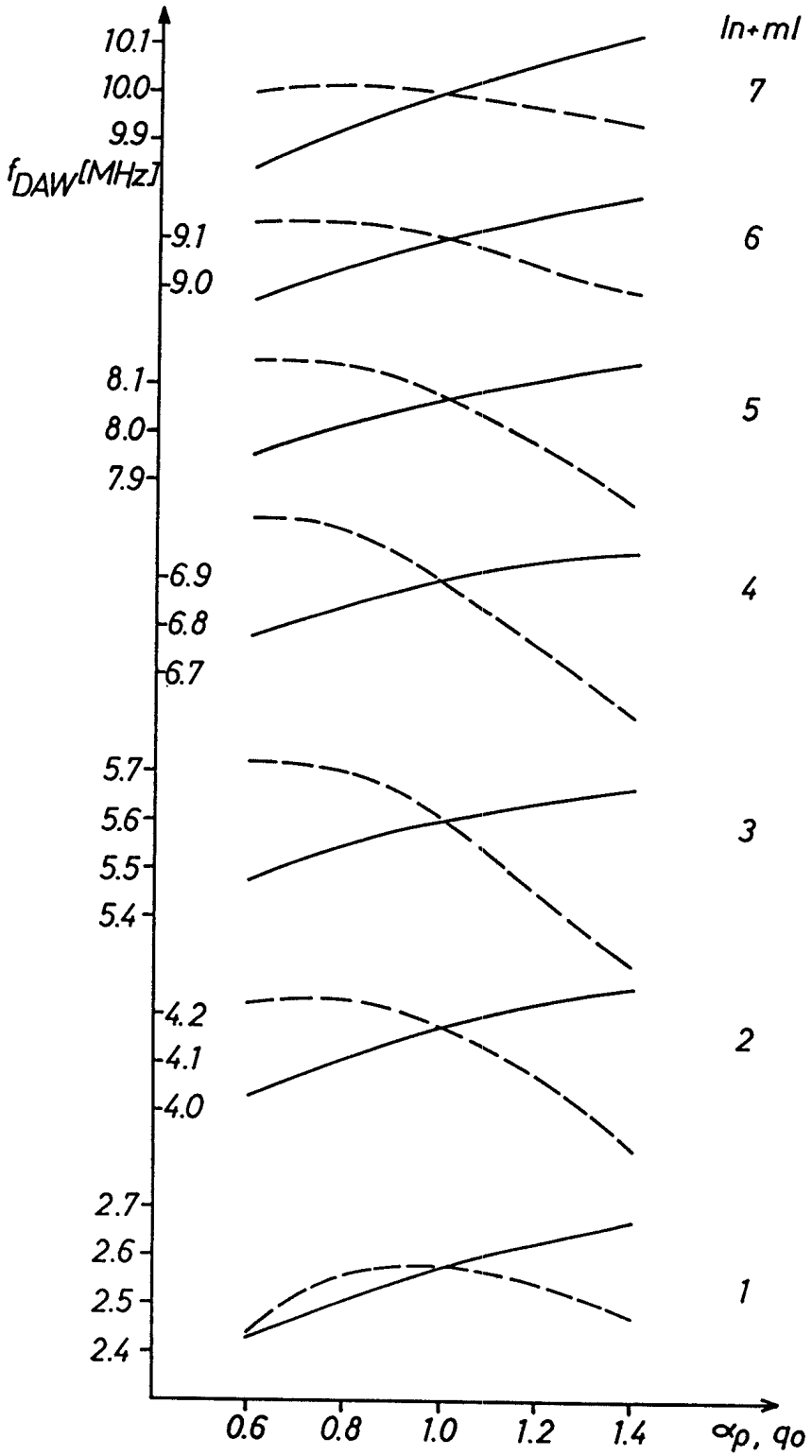
10.1
10.0
9.9
f_{DAW}[MHz]
9.1
9.0
8.1
8.0
7.9
6.9
6.8
6.7
5.7
5.6
5.5
5.4
4.2
4.1
4.0
2.7
2.6
2.5
2.4
0.6
0.8
1.0
1.2
1.4
α_p, q_0
|n+m|
7
6
5
4
3
2
1

FIG. 8

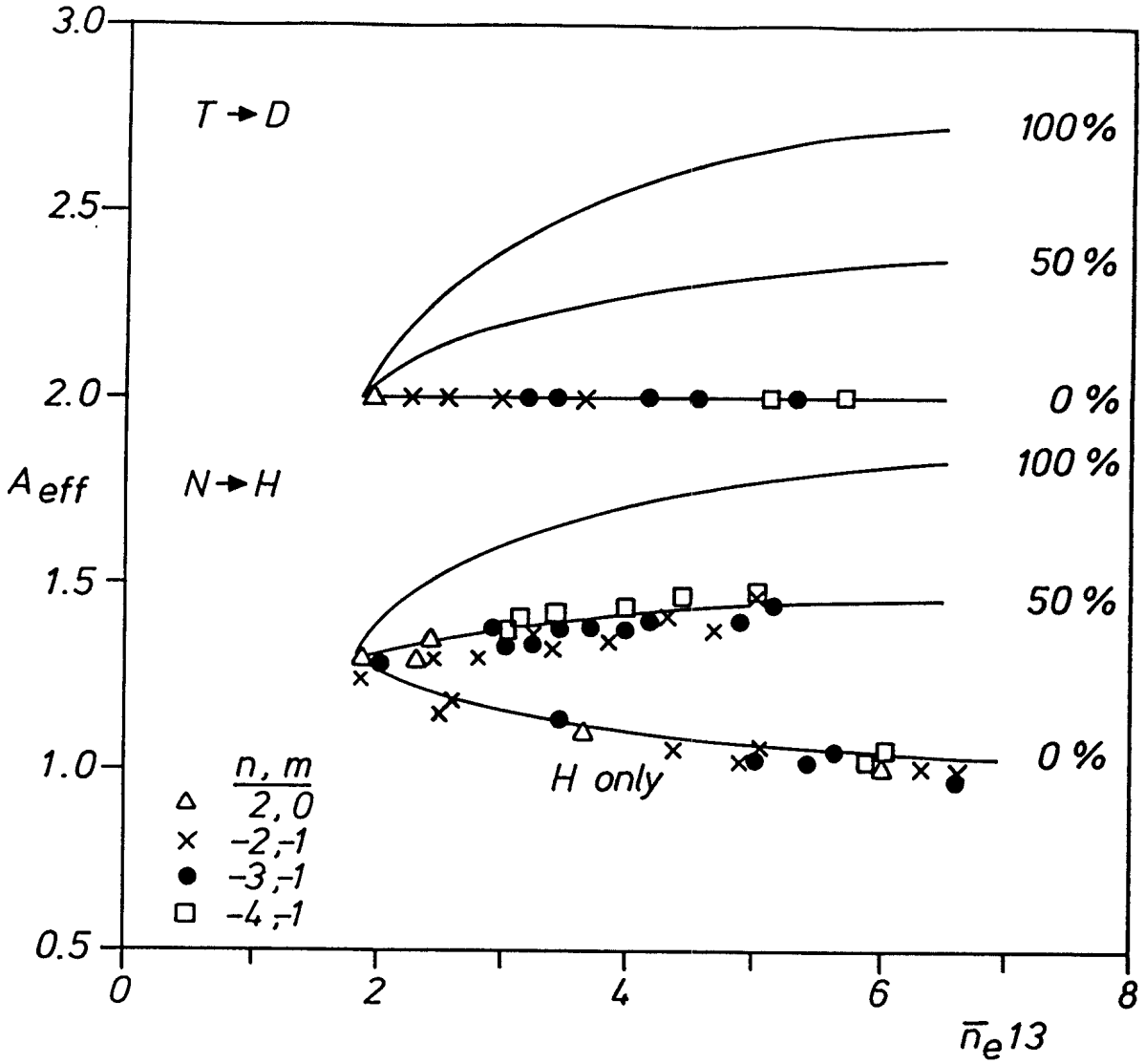
3.0
2.5
2.0
1.5
1.0
0.5
A_{eff}
T → D
N → H
100 %
50 %
0 %
100 %
50 %
0 %
H only
n, m
2, 0
-2, -1
-3, -1
-4, -1
0
2
4
6
8
$\bar{n}_e 13$

FIG. 9

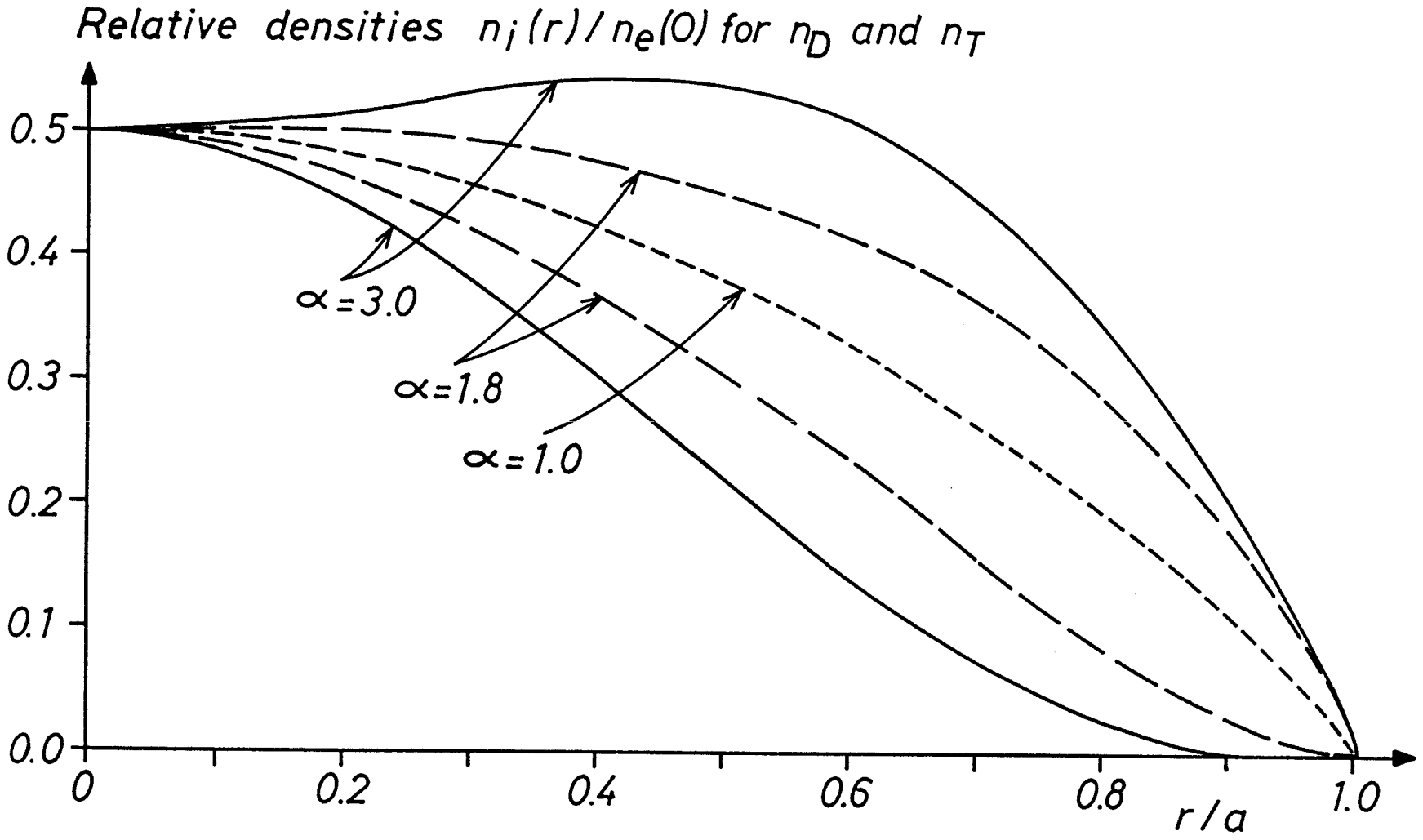
Relative densities $n_i(r)/n_e(0)$ for n_D and n_T
0.5
0.4
0.3
0.2
0.1
0.0
0
0.2
0.4
0.6
0.8
1.0
r/a
α=3.0
α=1.8
α=1.0

FIG. 10

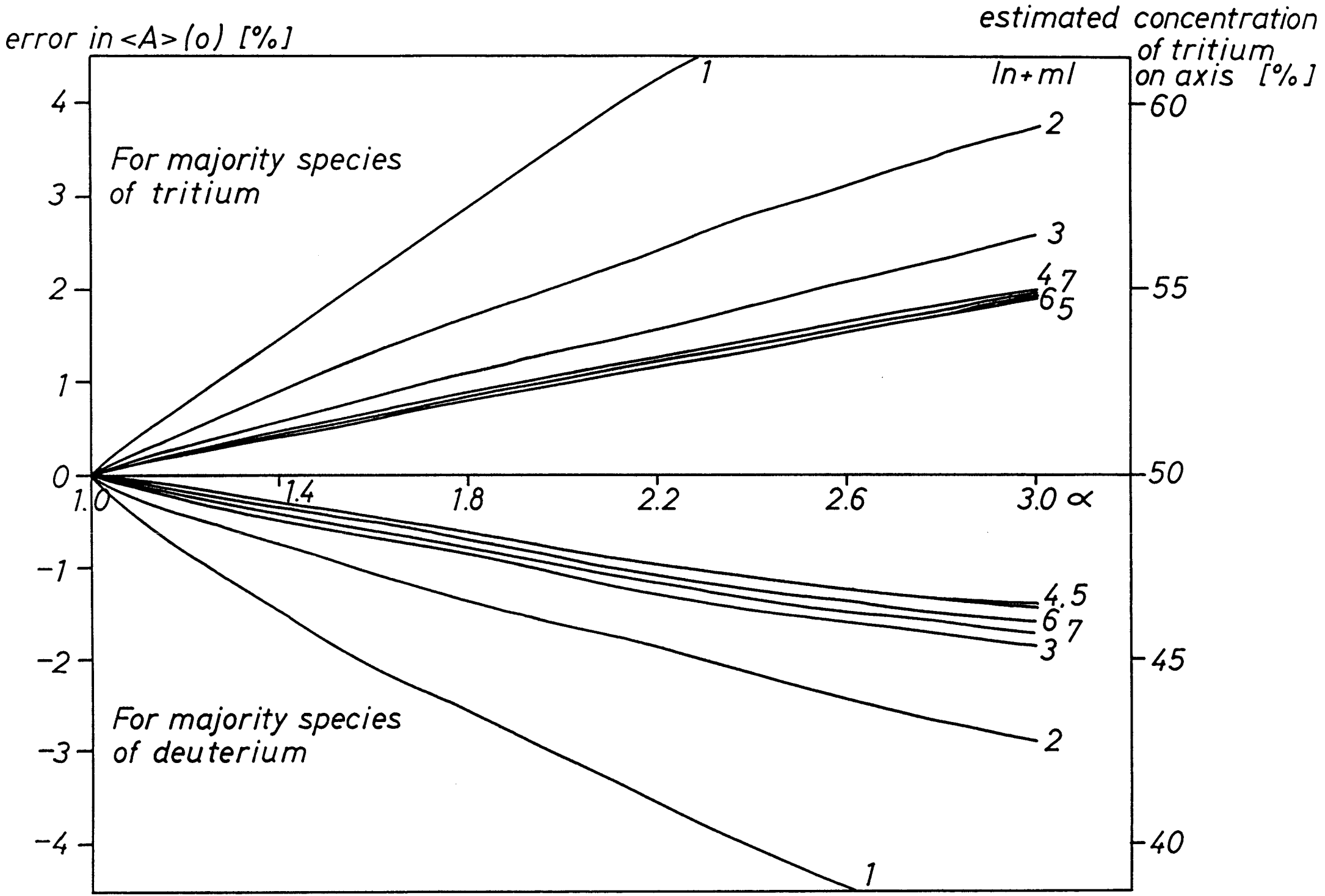
error in <A> (o) [%]
estimated concentration of tritium on axis [%]
ln+ml
For majority species of tritium
For majority species of deuterium
4
3
2
1
0
-1
-2
-3
-4
60
55
50
45
40
1.0
1.4
1.8
2.2
2.6
3.0 ∝
1
2
3
4 7
6 5
4.5
6 7
3
2
1

FIG. 11

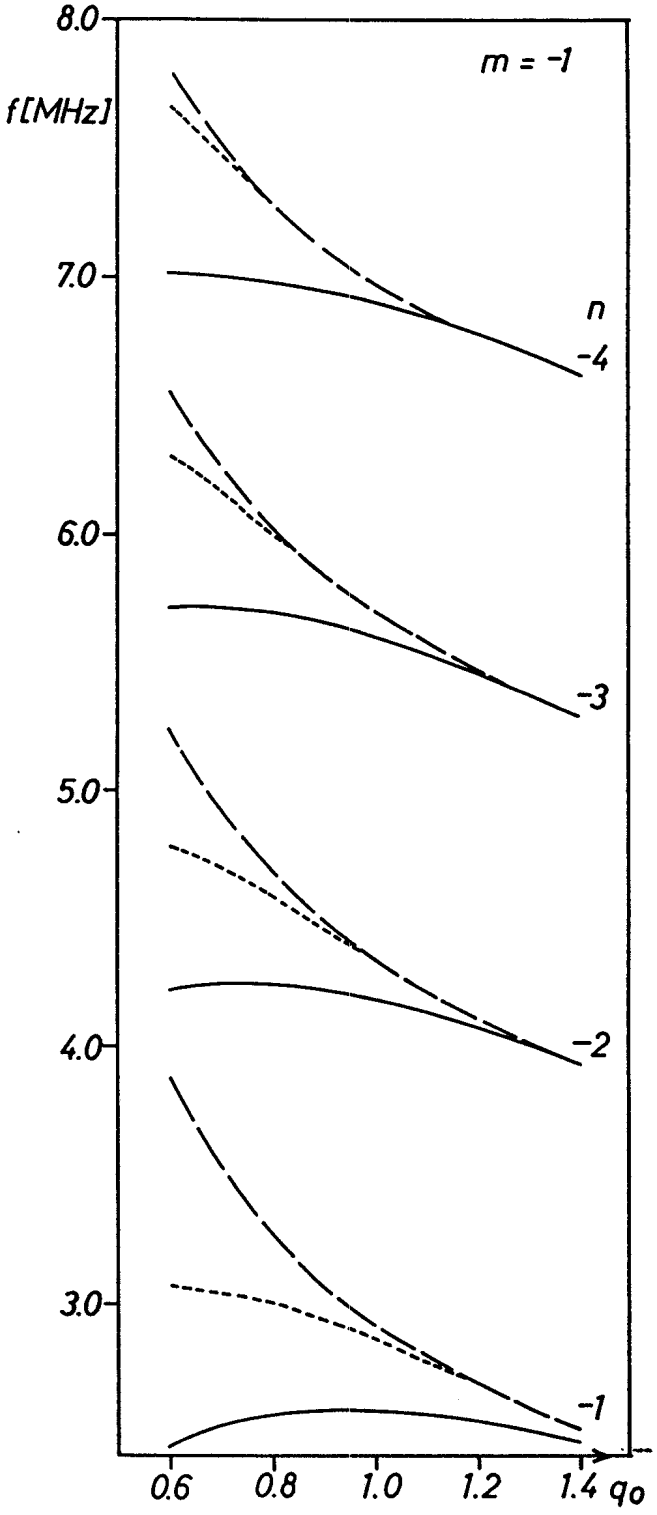

FIG. 12 A

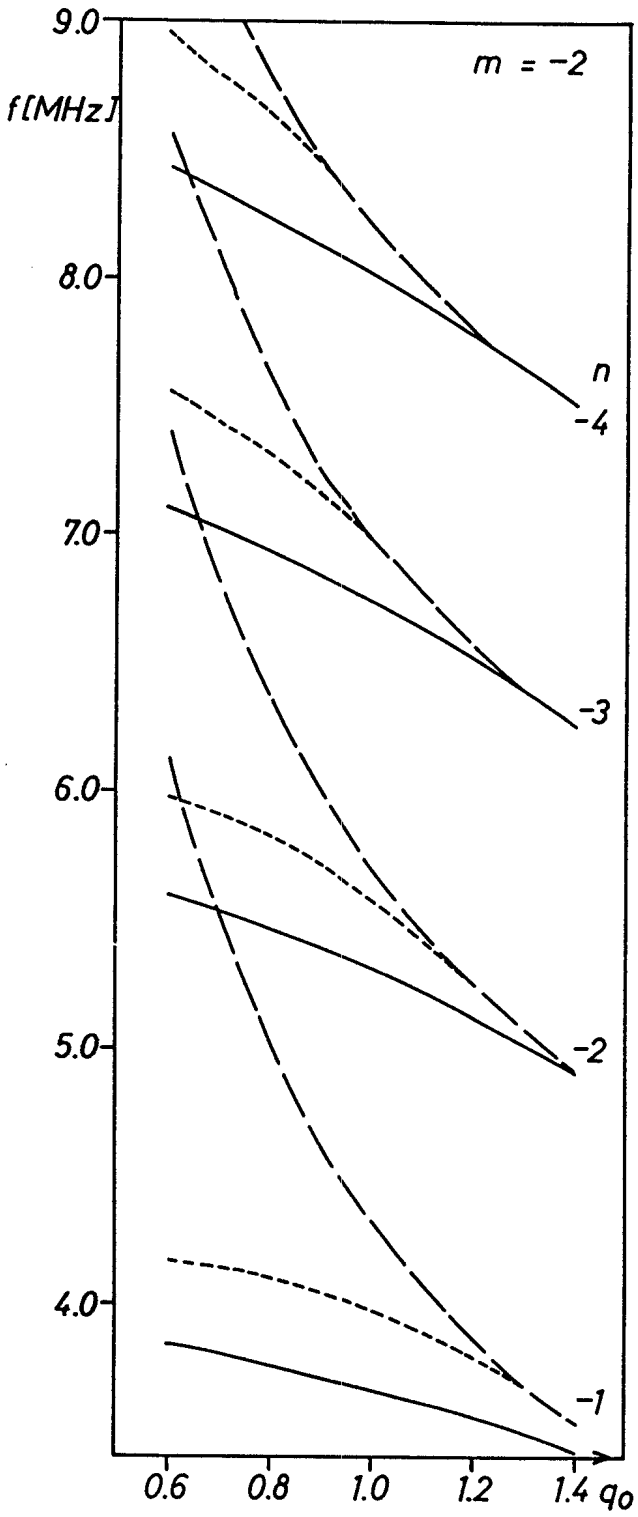

FIG. 12 B

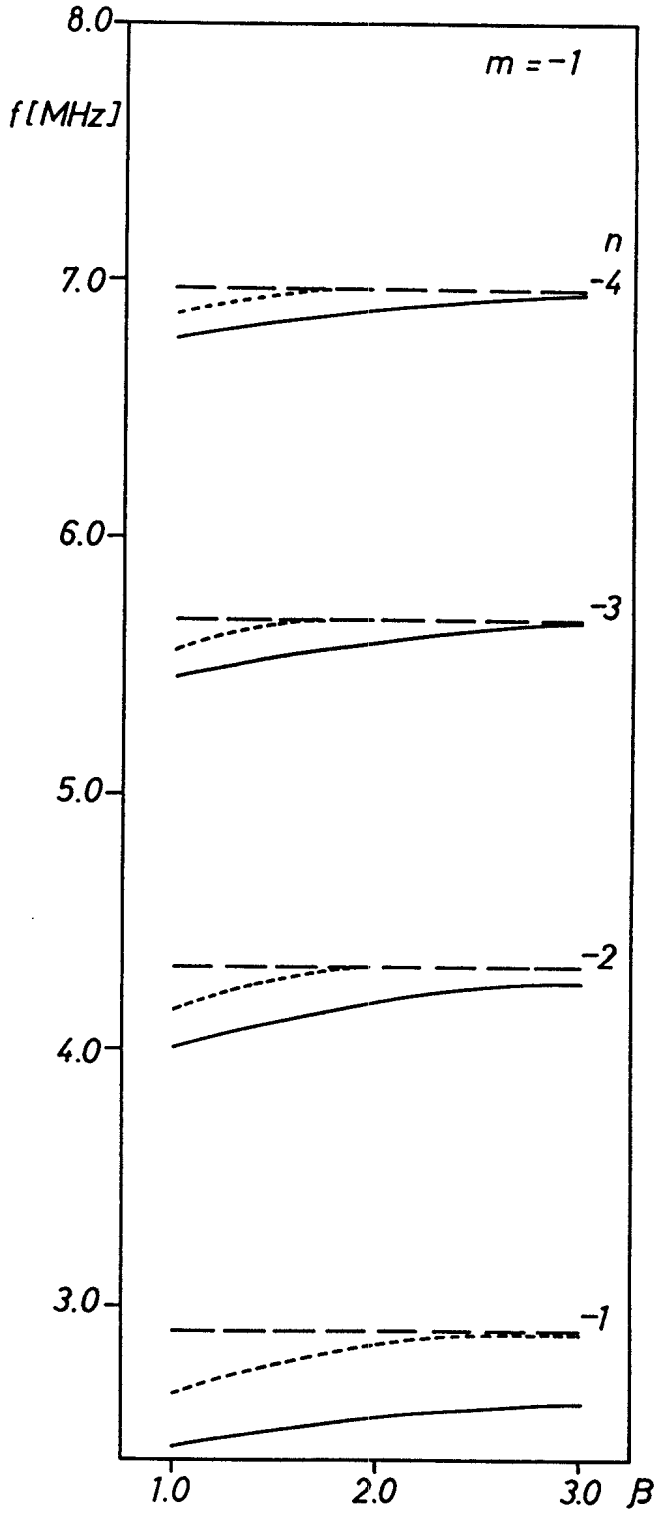

FIG. 13 A

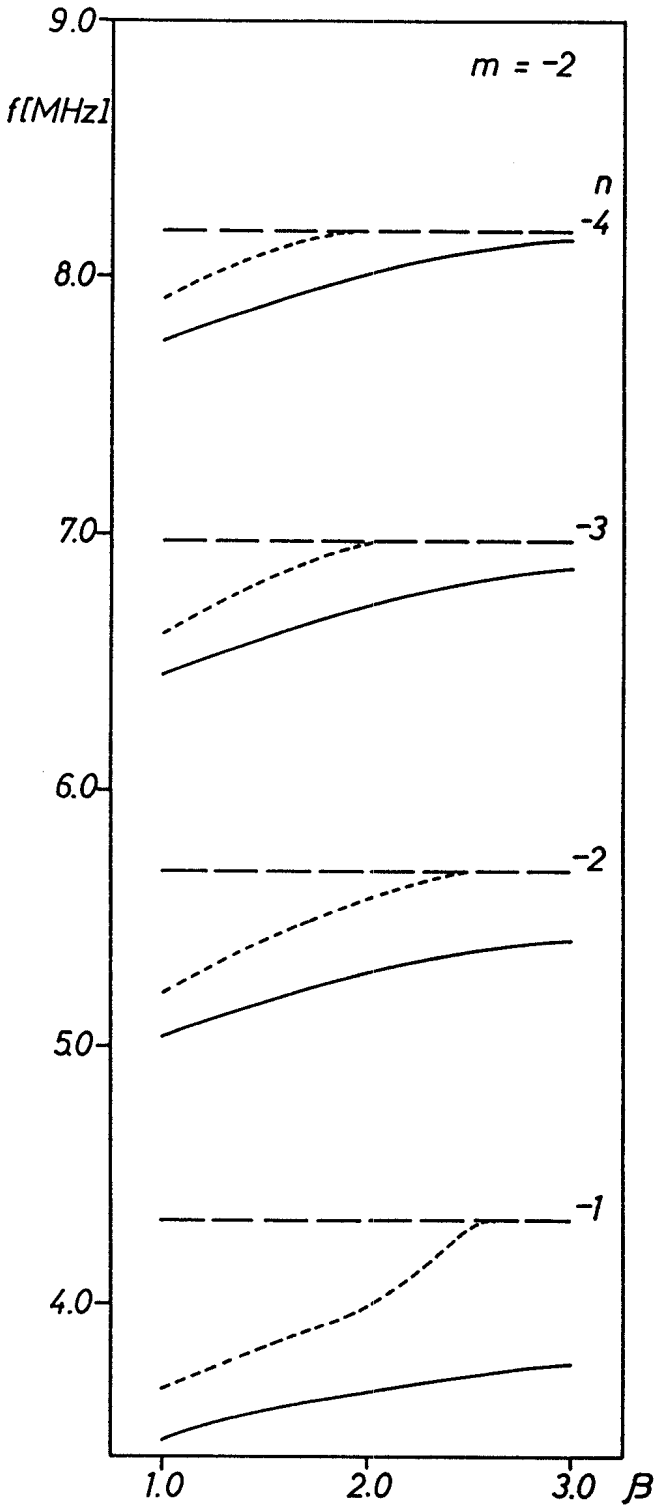

FIG. 13 B

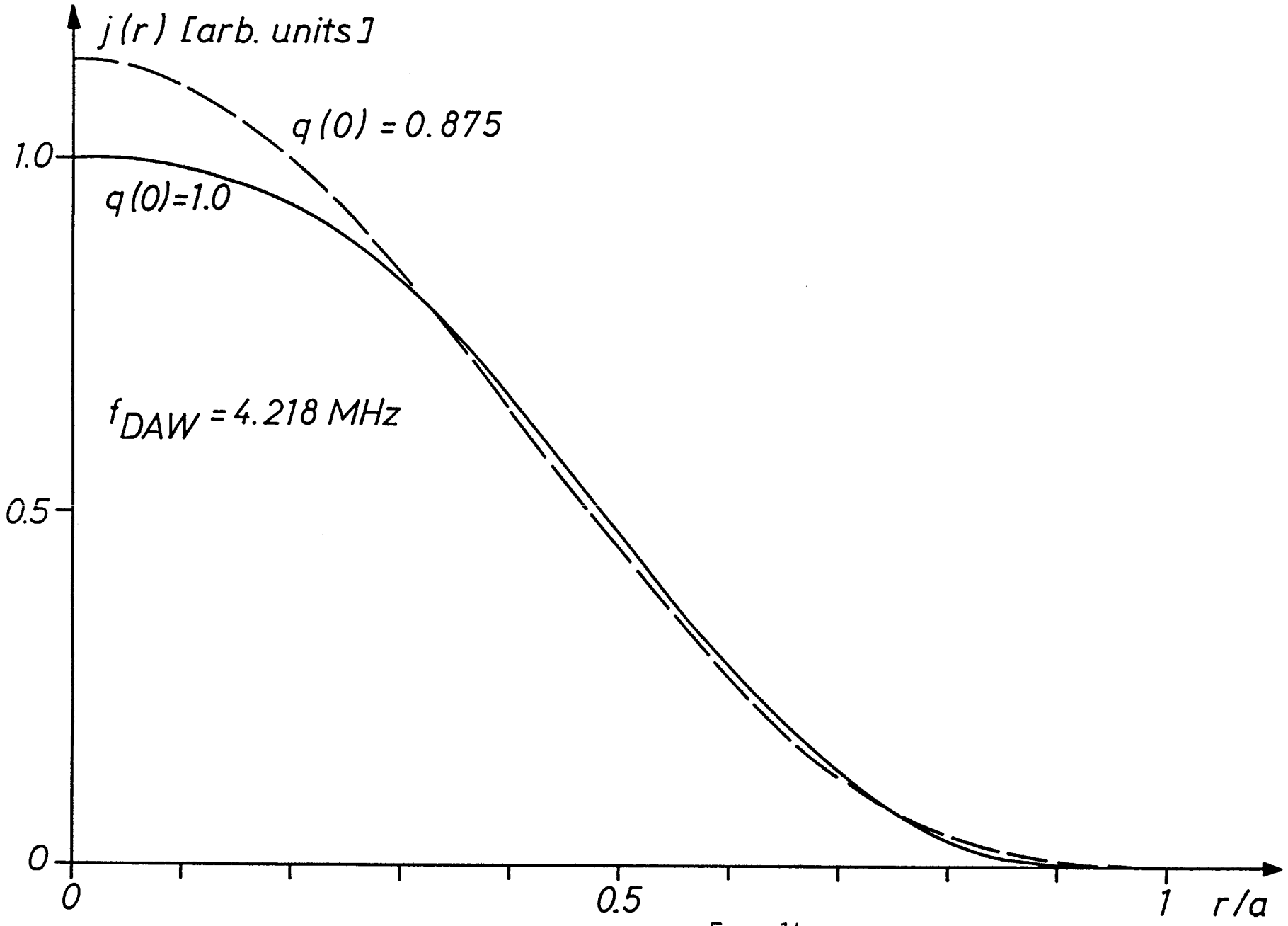

FIG. 14A

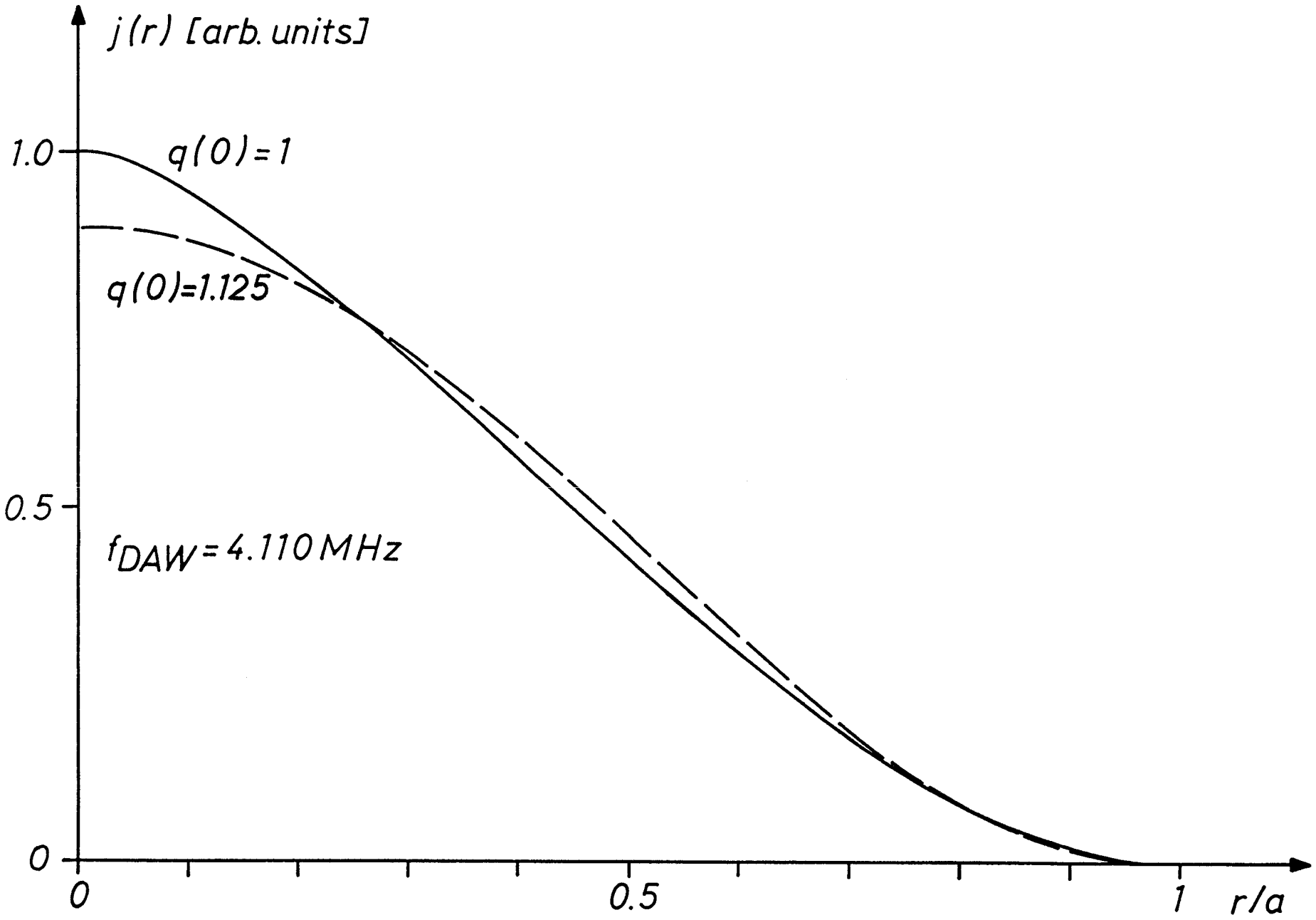

FIG. 14B

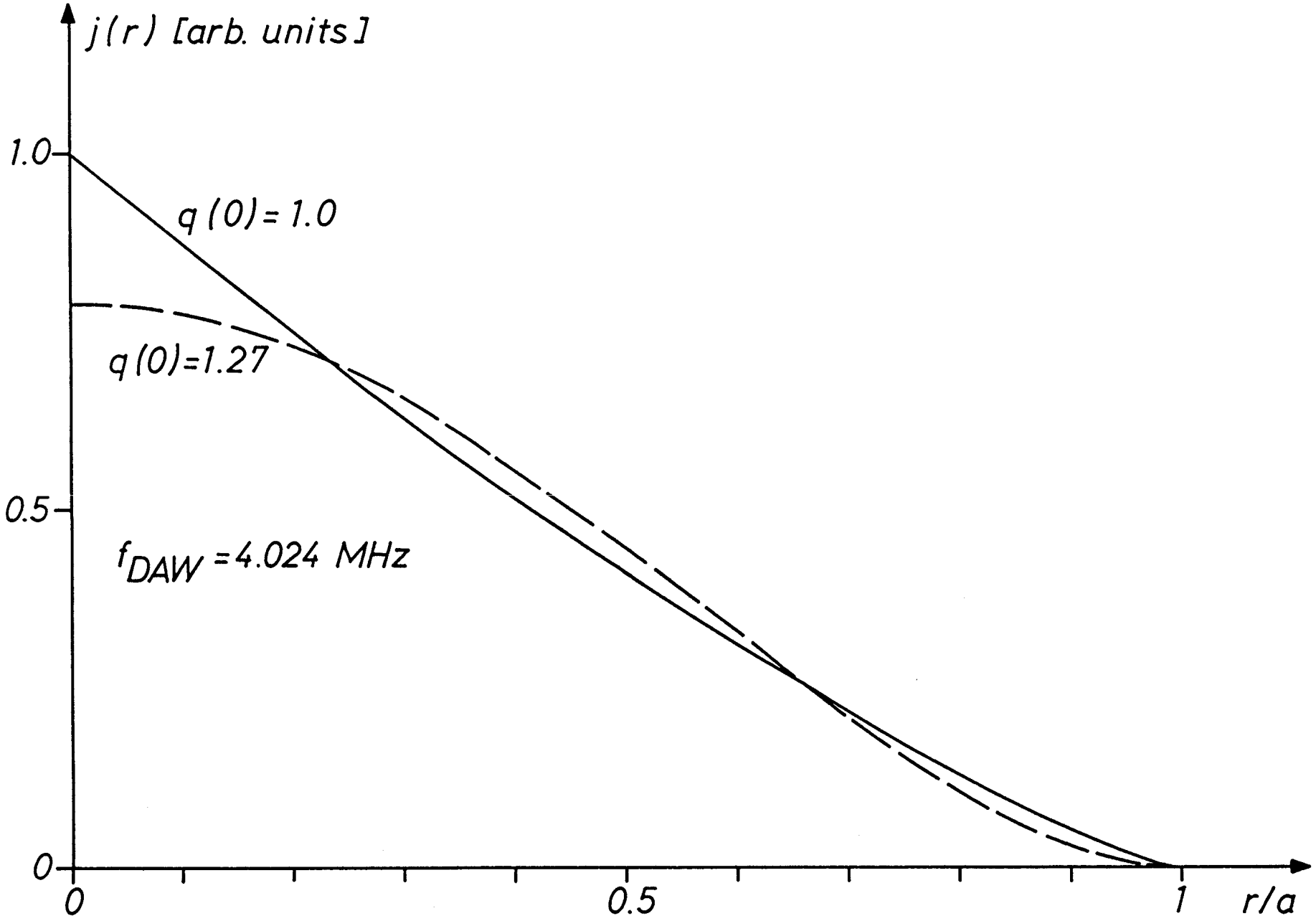

FIG. 14C

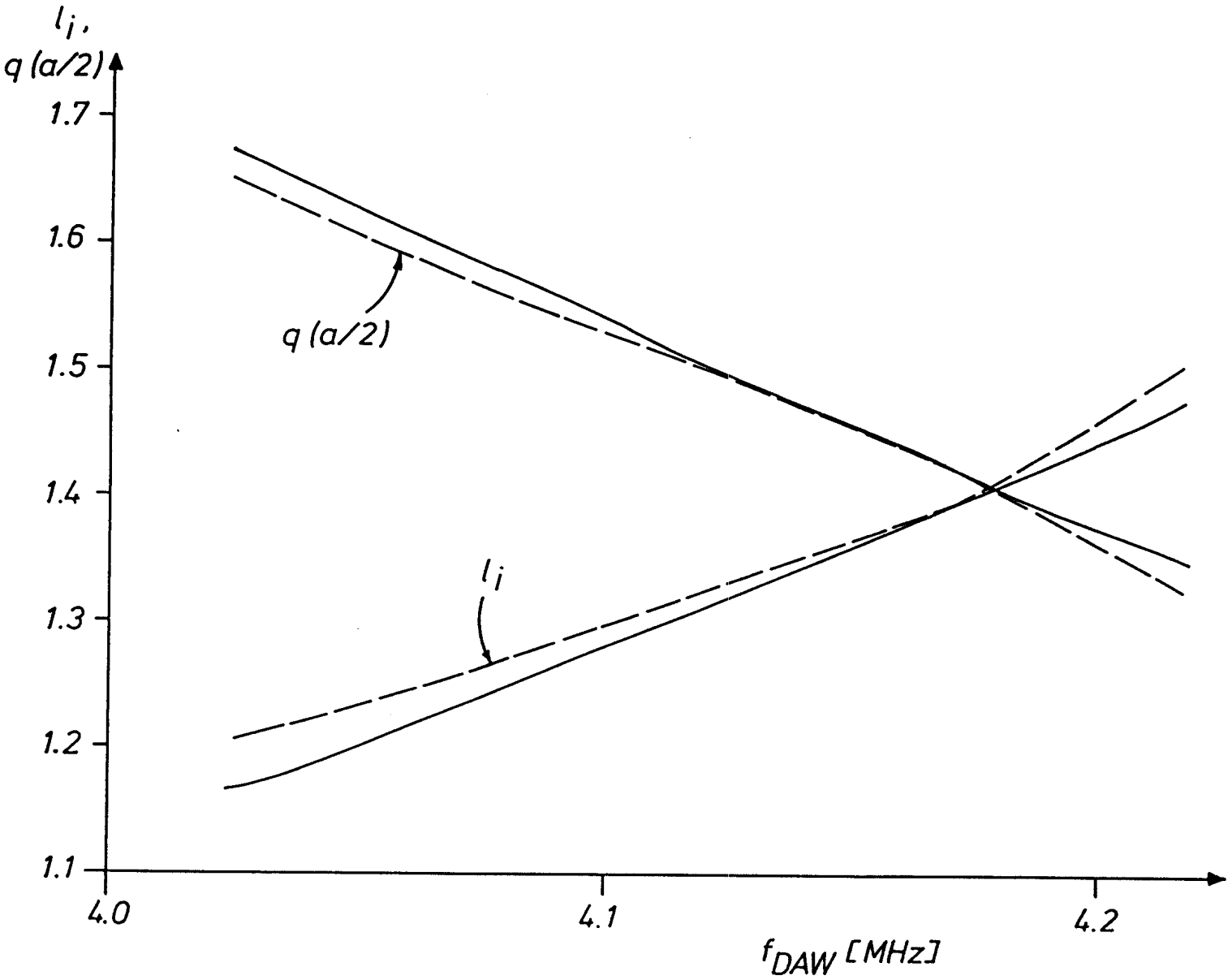

FIG. 15

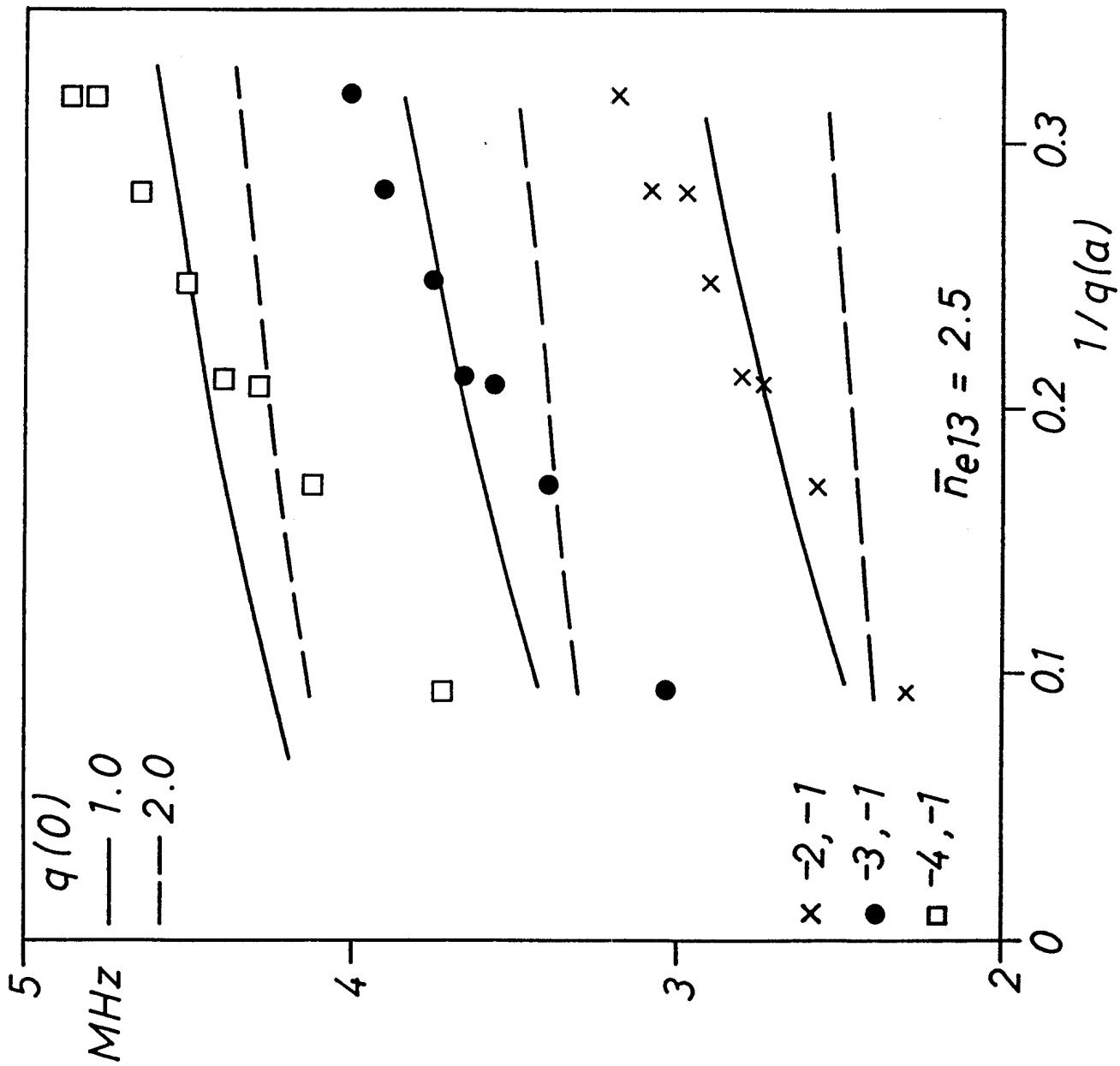

FIG. 16

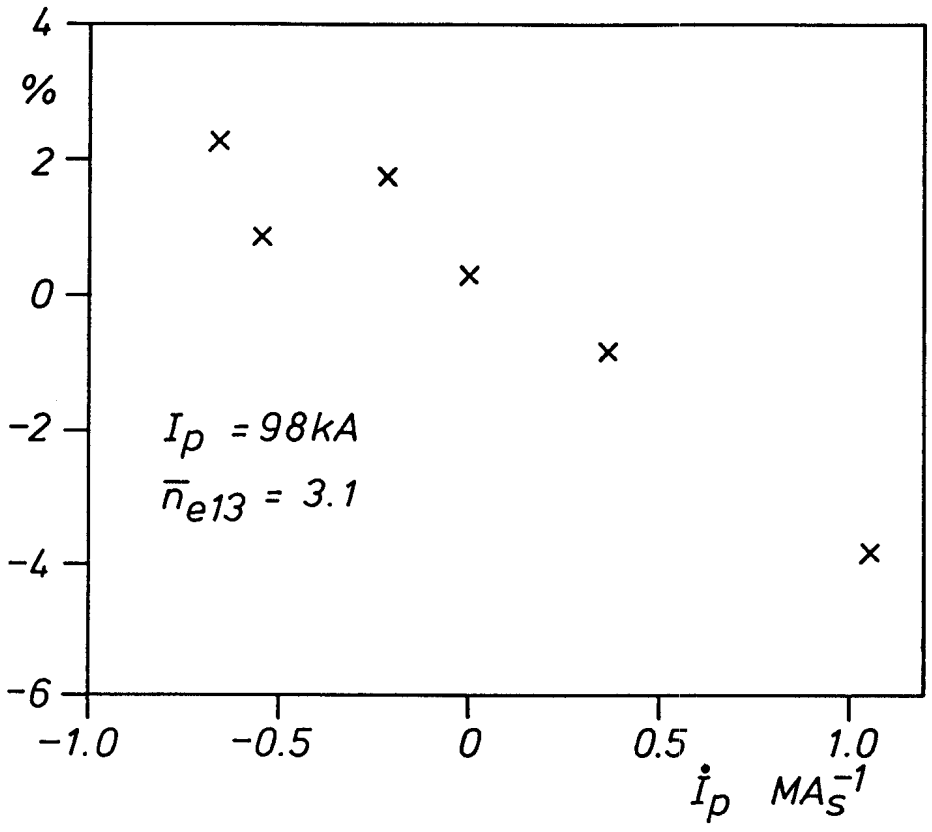

FIG. 17